Mizuno, T., T. Ohmori, and T. Akimoto. *Generation of Heat and Products During Plasma Electrolysis*. in *Tenth International Conference on Cold Fusion*. 2003. Cambridge, MA: LENR-CANR.org. This paper was presented at the 10th International Conference on Cold Fusion. It may be different from the version published by World Scientific, Inc (2003) in the official Proceedings of the conference.

Generation of Heat and Products During Plasma Electrolysis

Tadahiko Mizuno, Tadayoshi Ohmori and Tadashi Akimoto
Hokkaido University, Kita-ku Kita-13 Nishi-8, Sapporo 060-8628, Japan
E-mail: mizuno@qe.eng.hokudai.ac.jp

Abstract: Direct decomposition of water is very difficult to achieve in normal conditions. Hydrogen gas can be usually obtained by electrolysis and a pyrolysis reaction at high temperatures above 3700 degrees Celsius. However, as we have already reported, anomalous heat generation during plasma electrolysis is relatively easy to obtain under the right simultaneous conditions of high temperature and electrolysis. In this paper we discuss the anomalous amount of hydrogen and oxygen gas generated during plasma electrolysis. The generation of hydrogen in amounts exceeding Faraday's law is continuously observed when the conditions such as temperature, current density, input voltage and electrode surface are suitable. Non-Faradic generation of hydrogen gas is sometimes 80 times higher than the gas from normal electrolysis. Excess hydrogen has proved difficult to replicate by other laboratories, although we are able to reproduce it regularly.

Key word: plasma electrolysis, pyrolysis, hydrogen generation, current efficiency

1. Introduction

Hydrogen gas can be easily obtained by the electrolysis. However, direct decomposition of water is very difficult in normal condition. The pyrolysis reaction occurs at high temperatures above 3700 degrees Celsius (1, 2). We have already reported anomalous heat generation during plasma electrolysis (3, 4). Some researchers have attempted to replicate the phenomenon, but it has been difficult for them to generate large excess heat. They have tended to increase voltage to a very high value, around several hundred volts, but they measured no excess heat.

We observe anomalous hydrogen and oxygen gas generation during plasma electrolysis. The generation of hydrogen, which exceeds the Faraday law, is continuously observed when the conditions such as temperature, current density, input voltage and electrode surface are suitable. Sometimes this non-Faradic generation of hydrogen produces 80 times more hydrogen than normal electrolysis would. The plasma state itself can usually be triggered fairly easily, when the input voltage is increased to 140V or above at rather high temperature electrolysis cell (5, 6, 7). When the plasma forms, a great deal of vapor and the hydrogen gas is released from the cell. This effluent gas removes much of the energy from the cell, and with most conventional calorimeters this energy is not measured. This makes it difficult to calibrate, and to establish the exact heat balance. This simultaneous heat release and the gas release are complicated and difficult to measure. In this paper we show that anomalous hydrogen gas generation occurs during plasma electrolysis. We will describe a heat measurement technique used during the plasma electrolysis to capture all energy. This is important tool when replicating excess heat and other products during plasma electrolysis.

2. Experiment

2.1 Electrolysis cell

Figure 1 shows the experimental set up. We can measure many parameters simultaneously: sample surface temperature, neutron and x-ray emission, the mass spectrum of gas and input power and so on.

Figure 2 shows a schematic sketch of the cell and measurement system (1-2). The cell made of the Pyrex glass, 10 cm diameter and 17 cm in height, 1000 ml capacity. A cap made of Teflon rubber was installed in the cell. It is 7 cm in the diameter. The cap has several holes, three for platinum resistance temperature probes (RTD), two for tube carrying flowing coolant water tube (the inlet and outlet), and one for a tube to capture effluent hydrogen and oxygen gas, made of quartz, 5 cm in diameter and 12 cm in length. In

addition, the upper part of the tube is attached to a Teflon rubber cylinder with a water-cooled condenser built into it, as shown in Fig. 3 and photo 4.

2.2 Measurement of hydrogen gas

A dome or funnel-shaped quartz glass surrounds the cathode, extending below it. It is 5 cm in diameter, 12 cm in length. The effluent gas from the cathode — a mixture of hydrogen from electrolysis, hydrogen and oxygen from pyrolysis, and water vapor from the intense heat — is captured inside the funnel as it rises up to the surface of the electrolyte. After the gas rises to the top of the funnel, it passes through a Teflon sleeve into a condenser. The water vapor condenses and falls back into the cell, and the hydrogen and oxygen continues through an 8-mm diameter Tigon tube and a gas flow meter (Kofloc Corp., model 3100, controller model CR-700). This is a thermal flow meter; the flow detection element is a heated tube. The minimum detectable flow rate is 0.001 cc/s, and the resolution is within 1%. The gas flow measurement system is interfaced to a data logger, which is attached to a computer.

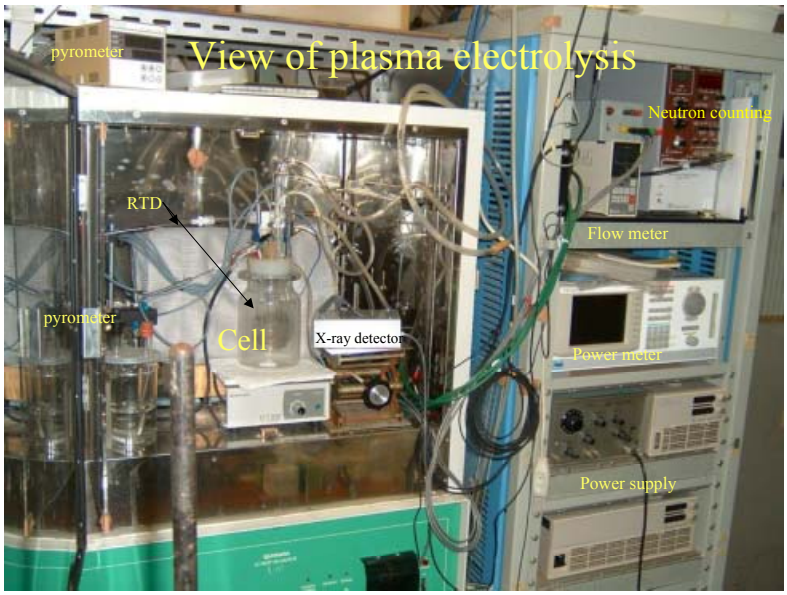

Fig. 1. Photo of the experimental set up

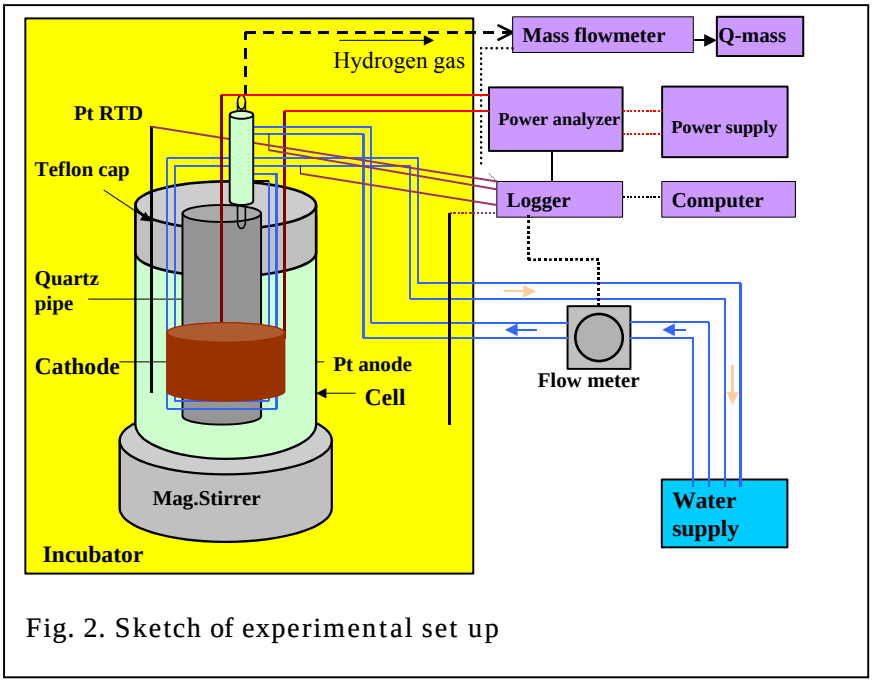

Fig. 2. Sketch of experimental set up

After passing through the flow meter, most of the gas is flushed into the air, but a small constant volume of the gas, typically 0.001 cc/s, is diverted to pass continuously through a needle valve and analyzed by a quadrupole mass spectrometer.

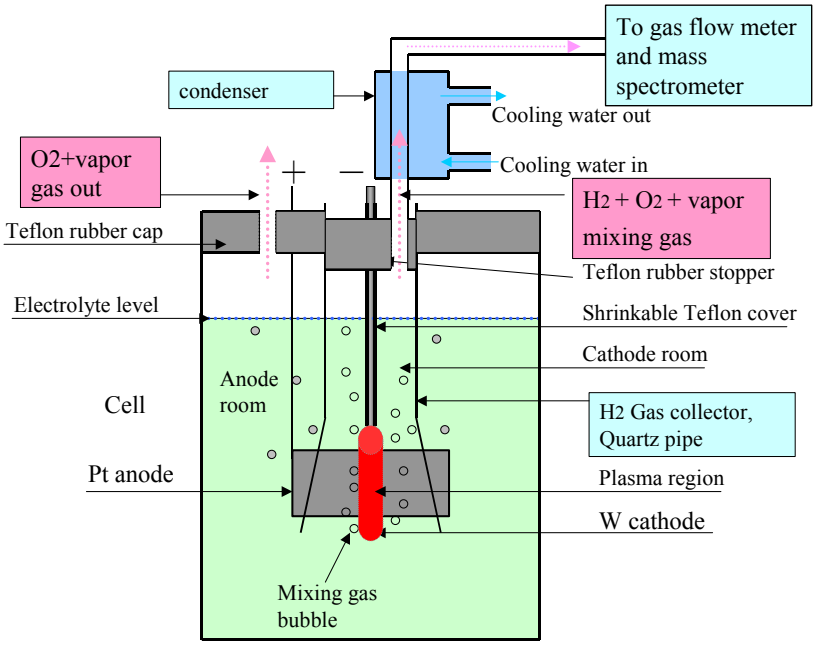

Fig. 3. Detail of the gas measurement

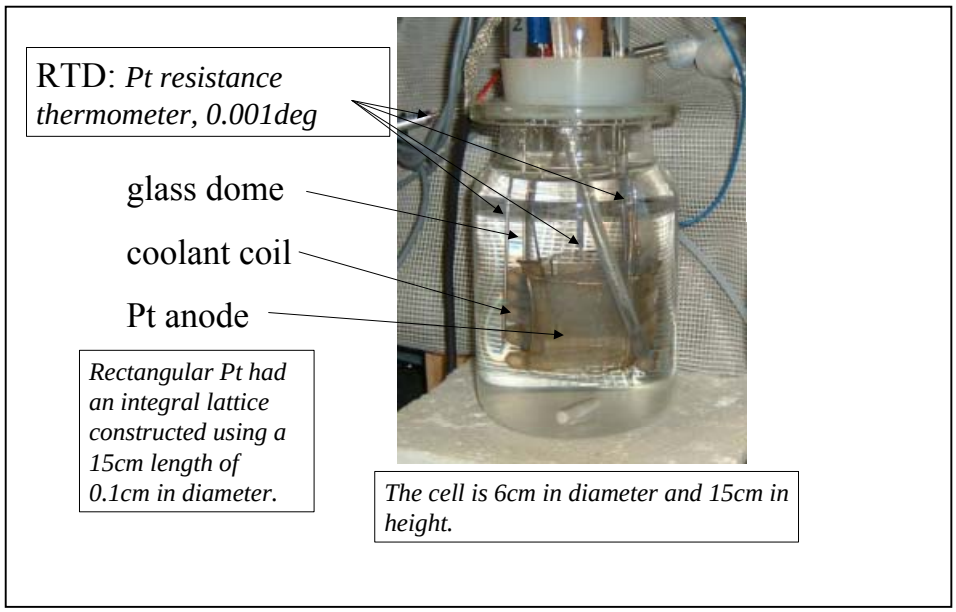

Fig. 4. Photo of cell

2.3 Calorimetry

As noted above, a quartz glass funnel surrounds the cathode. The anode is a mesh, wrapped around the outside of this funnel. A Teflon tube, in turn, is wrapped around the anode mesh, and cooling water flows through this tube. To summarize, the cathode is surrounded by a quartz glass funnel, the funnel outside surface is wrapped in the anode mesh, and a cooling water tube is coiled around the anode mesh. A platinum resistance temperature probes (RTD) is installed inside the tube, where the tube enters the cell system, and another RTD is installed where the tube exits the cell. (We call this the "system" here because after the cooling water passes the inlet RTD, it flows through the condenser above the cell, where it captures a great deal of heat, then it enters the Teflon tube in the cell, then finally it exits the cell and runs past the outlet RTD.) The temperature difference between the outlet and inlet RTDs is used to perform flow calorimetry on the cooling water.

Another set of three RTDs are mounted in the electrolyte, at different depths in the cell, to measure cell temperature and to perform isoperibolic calorimetry. A magnetic stirrer keeps the solution in the cell well mixed. The amount of the heat generation was determined by combining results from the flow and isoperibolic calorimetry and continuously comparing these two results with the input electric power.

Figure 5 shows the notional sketch of the heat measurement system. Heat out can be divided into several factors. These are: energy required for water decomposition; heat of electrolyte; heat removed by the coolant (the flowing cooling water in the Teflon tube); heat released from the call wall; and heat released with the vapor that exists through the cell plug outlet hole.

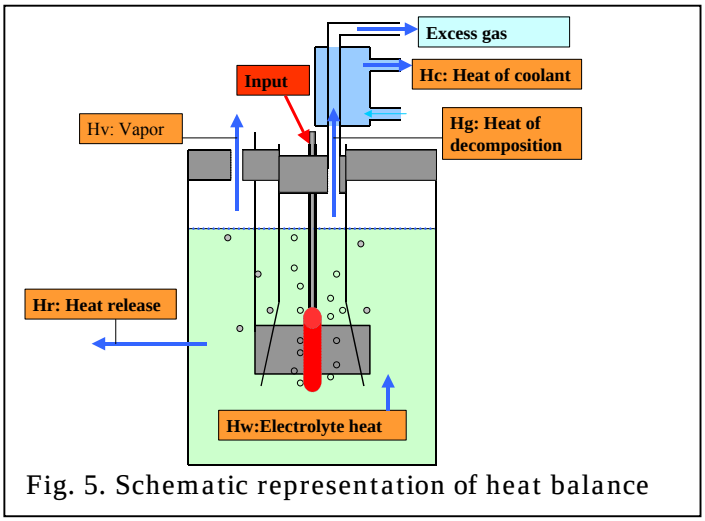

Fig. 5. Schematic representation of heat balance

The heat balance is determined for input and output two formulas:

· **Input** (J) = **I** (current) · **V**(Volt) · **t**
· **Out** = Hg + Hw + HC + Hr + Hv
here, Hg = Heat of decomposition = $\int 1.48 \cdot dI \cdot dt$
Hw = Electrolyte heat = $\int Ww \cdot Cw \cdot \delta T$
· *Ww*:electrolyte weight,*Cw*:heat capacity, δT:temperature difference
Hc = Heat of coolant = $\int Wc \cdot Cc \cdot \delta T$
· *Wc*:coolant weight, *Cc*:heat capacity, δT:temperature difference
· Hr = Heat release = $\int (Ww \cdot Cw + Wc \cdot Cc)Tr$
· *Tr:* temperature change
· Hv = vapor = $Wv \cdot Cc$

The calculation of the heat balance is relatively simple, despite the many factors that have to be taken into account. Input power is from the electric power source only. Output is divided to several parts. The first is Hg is heat of water decomposition. It is easily calculated from the total electric current. Hw is the electrolyte heat energy. It is also easy to calculate, based on the difference between the solution temperature and ambient. Hc is heat removed by the coolant. It is also easy to measure from the temperature difference between the coolant temperature at the inlet and outlet to the flow calorimetry system. The forth factor is Hr, heat release from the cell. This is rather complicated and can be determined by a semi-empirical equation. The fifth factor, Hv, is heat release by vapor from the cell. This is difficult to measure precisely. However, we have captured most of this heat directly by running the flow-calorimetry cooling water flow through the condenser.

If there is excess hydrogen and oxygen gas, we have to measure the gas volume precisely to determine how much energy it removes from the system. The equation for first factor, Hg, water decomposition was based on Faraday's law in the first approximation. It has to be changed to account for excess gas. The new equation can be based on the amount of hydrogen gas measured by the flow meter.

2.4 Electrode and solution

A tungsten wire 1.5 mm in diameter and 15 cm in length was used as the electrode, the upper 13 cm of the wire was covered with shrink-wrap Teflon, and the bottom 2 cm was exposed to electrolyte, and acted as the electrode. The light water solution was made from ultra high purity K_2CO_3 reagent at 0.2M concentration.

Fig. 6. W sample, before; left and after; right

Fig. 7. Photo of power supply

2.5 Power supply

A Takasago EH1500H supplied the electric power. Input power was calibrated for five seconds by a power meter (Yokogawa Co. model PZ4000). The sampling time was 40μs and the data length was 100k.

2.6 Thermometry

Temperature was measured with 1.5 mm diameter platinum resistance temperature probes (RTD) (Netsushin Co., model Plamic Pt-100Ω). The amount of the heat generation was calibrated by combined two methods with the flow calorimetric and isoperibolic by Pt sensors. Flow calorimetric was estimated from the temperature change of the water coolant that was once pass through a constant temperature bath through the Tigon tube from the tap water and the coolant mass was measured by a turbine meter.

2.7 Data accumulation

All data including the mass of cooling water flow from the flow calorimetry measurement, the temperature of coolant inlet and outlet, input voltage, current, integrated electric power and the amount of the hydrogen gas generated were collected by a data logger (Agilent Co., model 34970A). Moreover, the temperature data at locations in the cell electrolyte and the ambient temperature at one place in the thermostatic chamber were also collected by the logger. All data was finally collected in a computer.

2.8 element analysis

The sample electrodes and the electrolyte were subjected to element detection by means of energy dispersive X-ray spectroscopy (EDX), Auger electron spectroscopy (AES), secondary ion mass spectroscopy (SIMS) and electron probe micro analyzer (EPMA).

Fig. 8. Photo of EDX

Fig. 9. Photo of ICP mass

3. Result

We changed the input voltage stepwise as shown in Fig. 10. In this case, plasma electrolysis occurred at 120V. Once plasma formed, input current suddenly dropped. Meanwhile, the solution temperature rose to around 80 degrees. We then increased the voltage as stepwise to 350V, and then decreased it to 100V. Plasma continued at 100V and ceased at 80V.

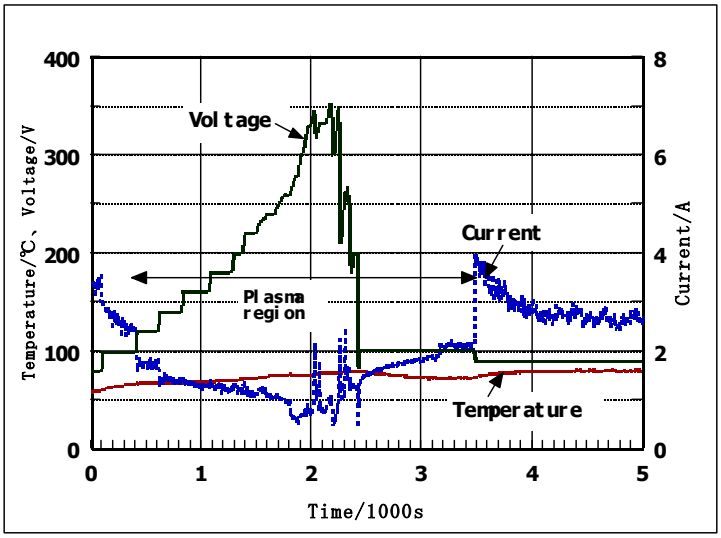

Fig. 10. Change for input voltage, current and Temperature

The gas captured in the cathode gas collector dome is calibrated by the Q-mass continuously, as shown in Fig. 11. It is mainly composed of the six gasses shown here. Other gases were under background levels and not detected after electrolysis started. Oxygen and nitrogen were detected throughout the measurement period. Oxygen increased after plasma electrolysis began, while other gases usually decreased. Hydrogen appeared when ordinary electrolysis started, and it decreased after the plasma electrolysis began. At the same time, oxygen increased. This oxygen level indicates that direct water decomposition started. Here, the behavior of the hydrogen isotope molecules is the same as the hydrogen molecular ion.

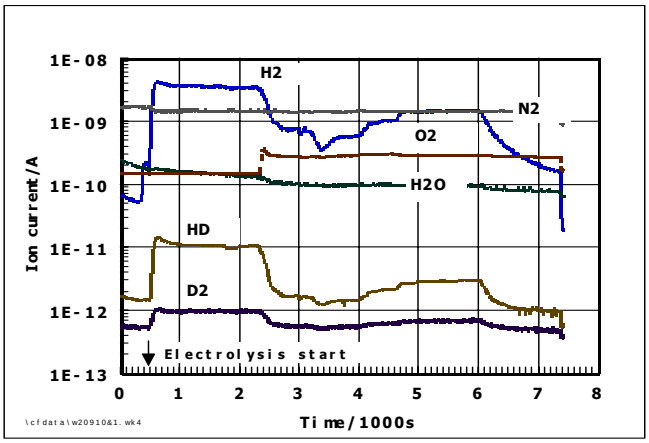

Fig. 11. Changes of the ion current of various masses

Figure 12 shows the time changes for hydrogen and oxygen molecules and their ratio. The ratio increase as input voltage increases. It is 0.45 at 2500s, at 350 V. This means the gas from the cathode was decomposed water. The ratio of the hydrogen in gases released from the cathode is exactly same as the value that indicated by the current. The equation is $(F_I\text{-}0.116I)*0.667+0.116I$. Here, F_I is the rate of hydrogen gas estimated from the flow meter and I is current. The factor of 0.116 is determined from the rate of ordinal hydrogen generation that is 0.5*22414/F (F; Faraday constant of 96500). And the factor of 0.667 is atomic ratio of hydrogen for water.

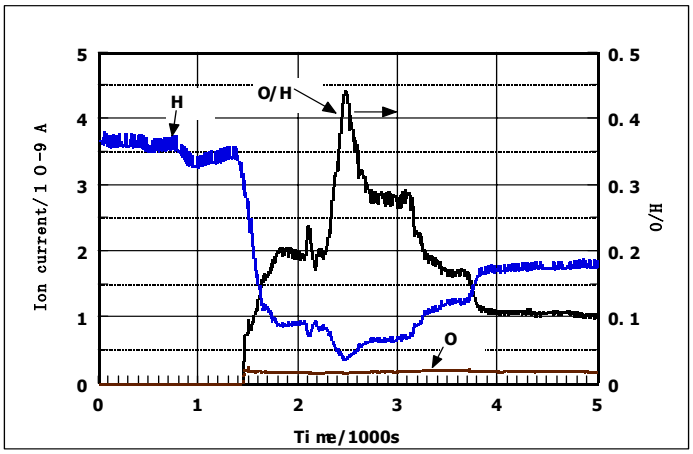

Fig. 12. Time changes of H2 and O2 ion current and the ratio

Figure 13 shows the changes of hydrogen generation estimated from the current and measured by the flow meter. These rates were the same in ordinary electrolysis. However, the value measured by the flow meter shows an upward deviation compared the value estimated from the current.

The change of the ratio between these two values, i.e., current efficiency (ε) and the ratio of the oxygen gas to the total generation with hydrogen from the cathode are shown in Fig. 4C. Here, the ε exceeded unity when plasma electrolysis started; gas generation increased a great deal with the input voltage. It reached as 8000% at 350V. The ratio of oxygen reached 30%. This means that almost all water decomposition in the cell was a caused by the high voltage plasma. In other words, pyrolysis decomposition occurred.

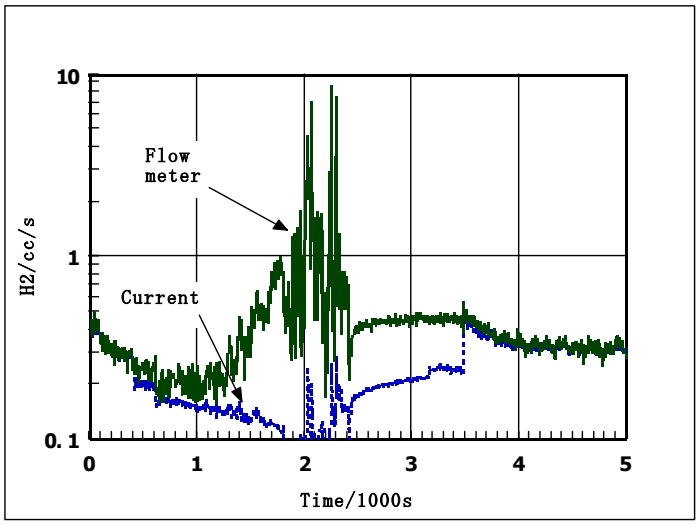

Fig. 13. Time changes of hydrogen generations

Figure 14 shows the change of the ratio between these two values, i.e., current efficiency (ε) and the ratio of the oxygen gas to the total generation with hydrogen from the cathode. Here, the ε exceeded unity when plasma electrolysis started; the gas generation increased a great deal as input voltage rose. It reached 8000% at 350V of input voltage. The theoretical value of hydrogen generation calculated from the input current was 1144 cc, and the measurement value during plasma electrolysis was 2190 cc. That is, the generation of excess hydrogen during a whole electrolysis run reached 1046 cc. If we consider only hydrogen generated during plasma conditions, the measured value was 1470 cc, the theoretical value is 460, and the excess is 1010 cc.

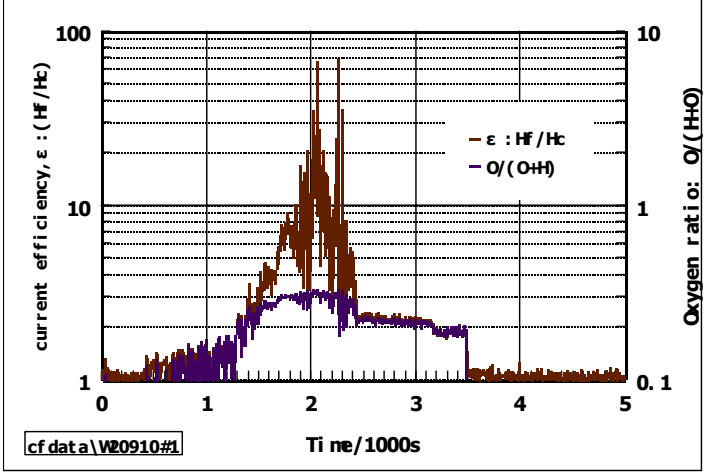

Fig. 14. Current efficiency and ratio of oxygen

Figure 15 shows the ε and V relationship. Here, it can be shown that ε has a tendency of increase with input voltage. Some points of ε value under 100V in the figure show up to twice of the theoretical value of unity; these points were obtained during plasma electrolysis. On the other hand, ε remains at unity for all of the normal electrolysis runs. It can be expected that if the input voltage were increased to several hundred V, then ε would far exceed unity.

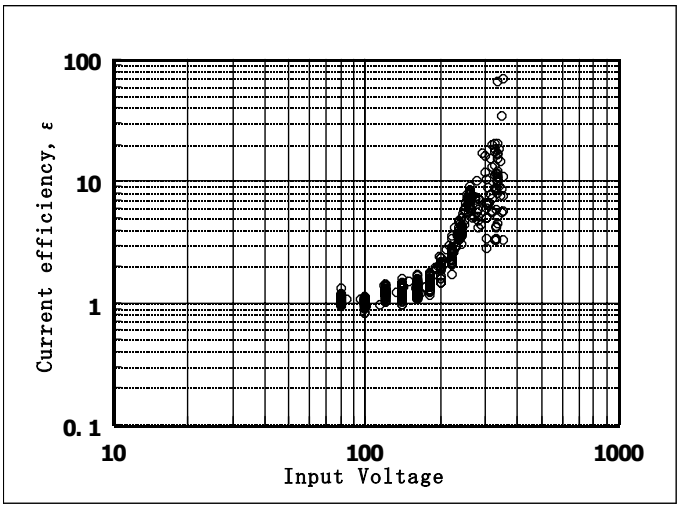

Fig. 15. Voltage dependency of current efficiency

Figure 16 also shows the ratio of excess hydrogen to input power. These values were subtracted from the faradic hydrogen shown in the previous graph, and converted to the equivalent energy. They show a steep increase with higher input voltage. The excess is greater than 10% and sometimes as high as 30%.

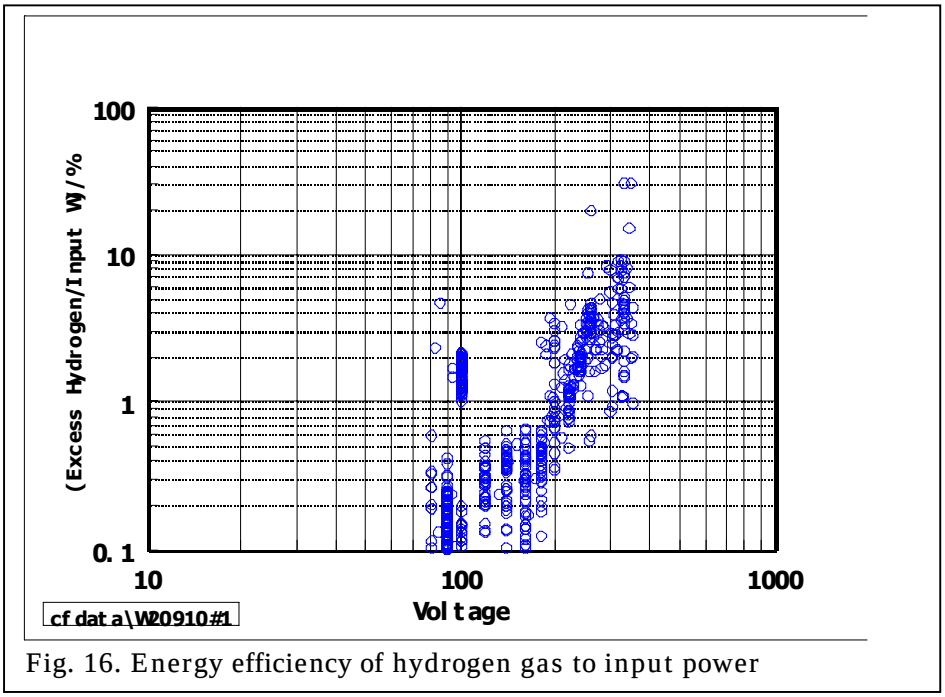

Fig. 16. Energy efficiency of hydrogen gas to input power

An example of heat generation is shown in Fig. 17. This shows no excess during the measurement. However, in this experiment, heat release with the oxygen evolution was not measured. So, it can be only said that in this case the heat balance was almost 100%.

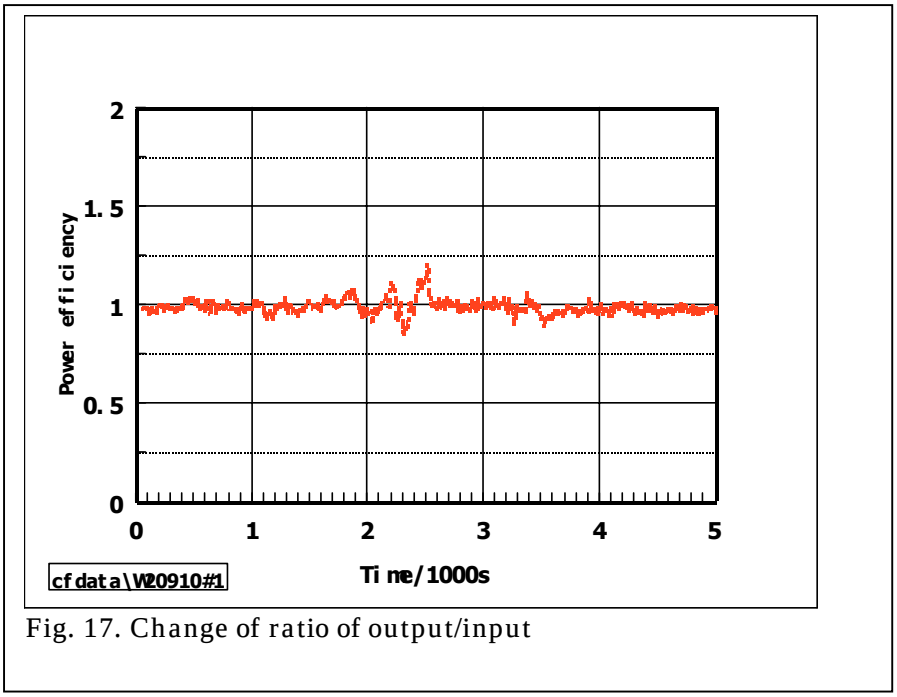

Fig. 17. Change of ratio of output/input

Figure 18 apparently shows the tendency of excess hydrogen generation to correlate with negative heat (an endothermic reaction). The total endothermic heat was calculated at 6540J during plasma electrolysis.

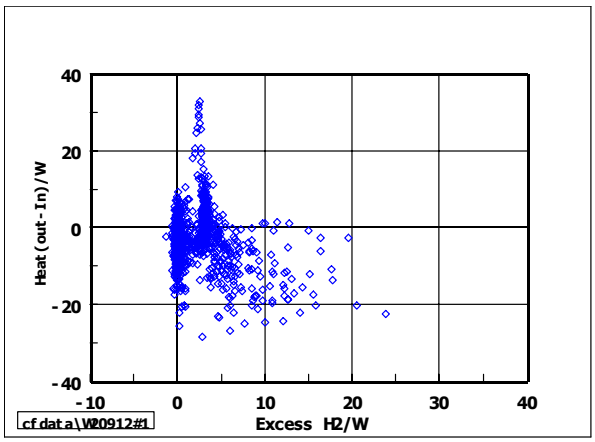

Fig. 18. Relation of heat balance and excess H2

When there is no excess heat, apparently the points for the excess hydrogen distribute around the no excess heat region as in Fig. 19, indicating the difference between heat out and electric power is zero.

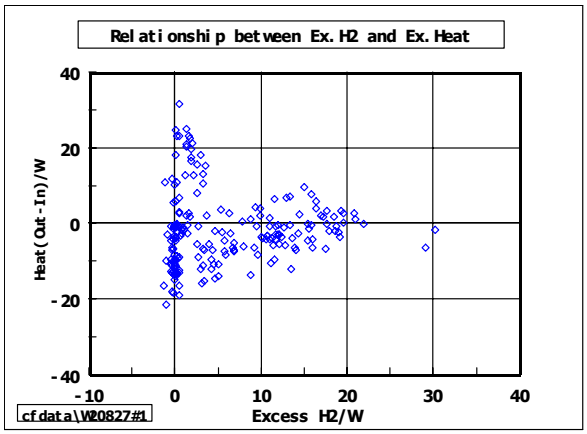

Fig. 19. Relation of heat balance and excess H2

Figure 20 shows a contrary relationship between excess hydrogen and excess heat. In this case, exothermic heat was estimated as 1100J during plasma electrolysis. In all three cases shown here, I accounted for the contribution of energy from excess hydrogen formation. However, the apparent heat balance was close to or below unity. It was affected by other parameters.

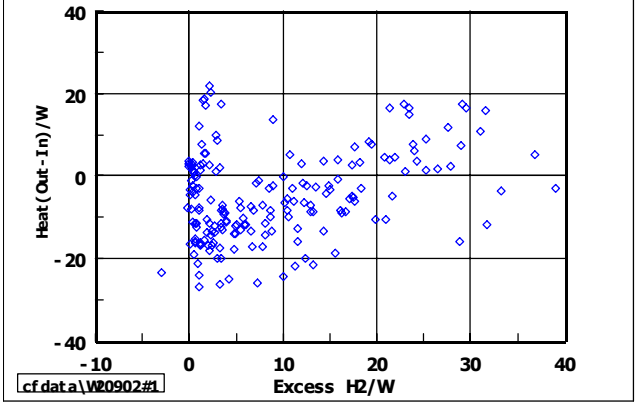

Fig. 20. Relation of heat balance and excess H2

We analyzed the elements in the electrode and the electrolyte by EDX and XPS method to estimate the entire distribution of elements in the electrolysis system. After electrolysis, the difference of the element deposition for these three cases were changed as indicated in Fig. 21. These depositions were also observed in various cases of the electrolysis systems (8, 9, 10, 11, 12).

There were several major elements observed in the systems when excess energy was released. These were Ca, Fe and Zn. And other hand, In and Ge were detected for the case of endothermic heat. However, we have no major elements detected in the system when no heat phenomenon occurred.

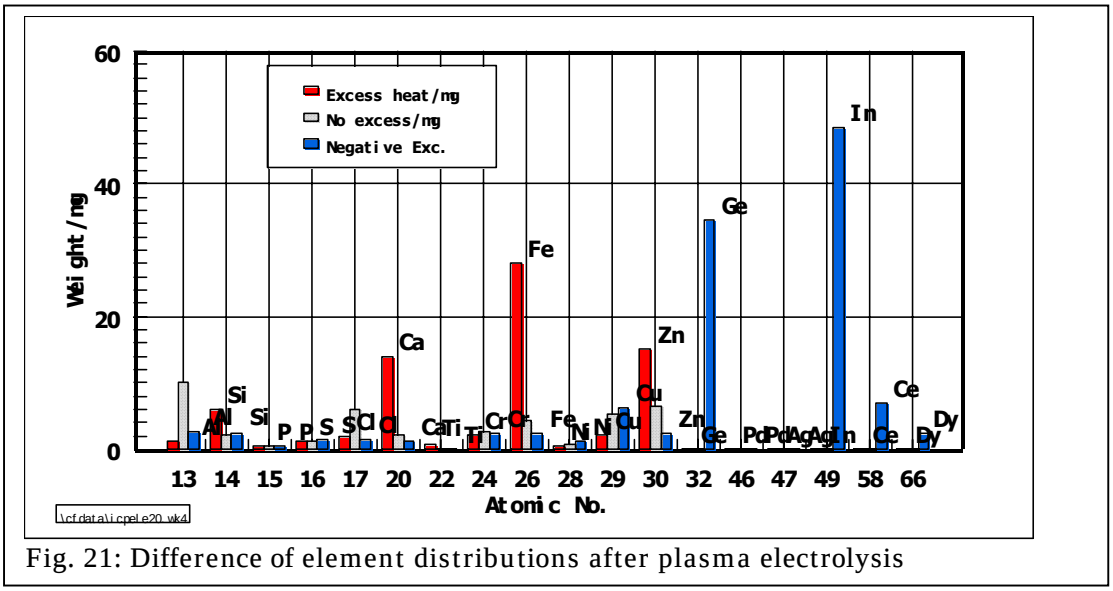

Fig. 21: Difference of element distributions after plasma electrolysis

4. Results

It is still difficult to determine what conditions are needed for excess energy generation. However, it is apparent that we must account for the contribution of the excess hydrogen to measure excess. Sometimes the excess hydrogen energy was as much as 30% of the input energy. This was in addition to excess heat already measured with calorimetry. However, duration of the excess energy generation only continued for several hundred seconds. One of the key factors controlling excess energy production seems to be input voltage. Hydrogen generation and heat generation seems to correlate with the input voltage. It can go over unity for the energy output during plasma electrolysis if the input voltage was kept very high. Apparently, we have replicated the phenomenon that the excess heat generation had been occasionally occurred at high input voltage region, even if the duration time was not enough long. One point of ε value in the figure shows up to 80 times of the theoretical value of unity; the point was obtained by the result of plasma electrolysis at 350V. On the other hand, the ε remains at unity for all of the other normal electrolysis. It can be expected that if the input voltage were increased to several hundred volts, the heat out would far exceed the value of unity.

5. Conclusions

1. Current efficiency for plasma electrolysis reaches 8,000% of the input current.
2. Power efficiency for plasma electrolysis reaches 30% to the input voltage.
3. In some cases, excess heat was observed.
4. In other cases, no excess endothermic heat were observed.
5. The reaction products after electrolysis were different when excess heat was generated.

References:

(1) Arakawa, H., "Creation of new energy by photocatalyst: Technology of clean hydrogen fuel production from solar light and water", Reza Kenkyu Vol.**25** (6), (1997) 425-430.

(2) Richard Rocheleau, Anupam Misra, Eric Miller, "Photo electrochemical hydrogen production", Proc., 1998 US-DOE, Hydrogen Program Review, NREL/CP-570-25315.

(3) Tadahiko Mizuno, Tadayoshi Ohmori, Tadashi Akimoto, Akito Takahashi, "Production of Heat during Plasma Electrolysis in Liquid", Jpn J. Appl. Phys., Vol.**39**, No.10 (2000) 6055-6061.

(4) T. Mizuno, T. Akimoto and T. Ohmori, "Confirmation of Anomalous Hydrogen Generation by Plasma Electrolysis", Proc. 4th meeting JCF research Soc., ed. H. Yamada, Oct., 17-18 (2002). Iwate Univ., Japan. (2002) 27-31

(5) A. Hickling and M. D. Ingram, Trans. Faraday Soc., Vol.**60** (1964) 783

(6) A. Hickling, "Electrochemical processes in glow discharge at the gas-solution Interface", Modern Aspects of Electrochemistry No.6, ed. by J. O'M. Bockris and B. E. Conway, Plenum Press New York (1971) 329-373

(7) S. K. Sengupta and O. P. Singh and A. K. Srivastava, J. Electrochem. Soc., Vol.**145** (1998) 2209

(8) Tadahiko Mizuno, Tadashi Akimoto, Tadayoshi Ohmori, Akito Takahashi, Hiroshi Yamada and Hiroo Numata, "Neutron Evolution from a Palladium Electrode by Alternate Absorption Treatment of Deuterium and Hydrogen", Jpn J. Appl. Phys, Part 2, No.9A/B, Vol.**40** (2001) L989-L991.

(9) Tadahiko Mizuno, Tadayoshi Ohmori and Michio Enyo, "*Anomalous Isotopic Distribution in Palladium Cathode After Electrolysis",* J. New Energy, 1996. **1**(2), p. 37.

(10) Tadahiko Mizuno, Tadayoshi Ohmori, Kazuya Kurokawa, Tadashi Akimoto, Masatoshi Kitaichi, Koichi Inoda, Kazuhisa Azumi. Sigezo Shimokawa and Michio Enyo, "*Anomalous isotopic distribution of elements deposited on palladium induced by cathodic electrolysis",* Denki Kagaku oyobi Kogyo Butsuri Kagaku, 1996. **64,** p. 1160 (in Japanese).

(11) Tadahiko Mizuno, Tadayoshi Ohmori and Michio Enyo, "*Isotopic changes of the reaction products induced by cathodic electrolysis in Pd",* J. New Energy, 1996. **1**(3), p. 31.

(12) Tadahiko Mizuno, Tadayoshi Ohmori and Michio Enyo, "*Confirmation of the changes of isotopic distribution for the elements on palladium cathode after strong electrolysis in D2O solutions",* Int. J. Soc. Mat. Eng. Resources, 1998. **6**(1), p. 45.